Earth Planet. Sci. Lett. 685 (2026) 120021

Contents lists available at ScienceDirect

Earth and Planetary Science Letters

journal homepage: www.elsevier.com/locate/epsl

Sediment supply controls on channel morphological adjustments to tectonics and lithology

Ziqiang Zhou [a,*], Reha Chandresh [b], Alexander C. Whittaker [a], Gary J. Hampson [a], Rebecca E. Bell [a]

[a] Department of Earth Science and Engineering, Imperial College London, London SW7 2AZ, UK
[b] Department of Earth Sciences, University of Florence, Florence 50121, Italy

ARTICLE INFO

Edited by: J.P. Avouac.

Keywords:
Channel geometry
Shear stress
Sediment supply
"Tools and cover" effect
Corinth

ABSTRACT

In nature, rivers not only incise bedrock but also transport sediment supplied to them; however, incision is often assumed to dominate over sediment transport in shaping channel geometry so as to exploit the simplicity of the stream power law. This likely flawed assumption raises fundamental concerns about inverting channel morphology to map external forcing, such as active deformation. Central to this issue is how relative sediment flux (i.e. sediment supply relative to transport capacity, *Qs/Qt*) modulates the efficacy of excess shear stress in incising bedrock, known as the relative sediment flux function. Two competing functions have been proposed, but resolving them in the field has proven challenging to date. Here, we address this issue by contrasting two rivers in the Gulf of Corinth, Greece that traverse comparable gradients in tectonics and lithology with distinct relative sediment fluxes. We show that the sediment-rich Phoenix river, with an estimated *Qs/Qt* value ~0.8, has a much lower sensitivity of excess shear stress to tributary sediment input than the sediment-poor Sithas river. To our knowledge, this represents the first field evidence supporting the function with a markedly decreased sensitivity to *Qs/Qt* at high *Qs/Qt* values. This allows us to clarify the importance and mechanisms of channel slope versus width adjustment in reaching the excess shear stress required for equilibrium. As a result, we outline the conditions under which the widely used stream power law and its associated metrics, such as steepness and knickpoints, can (or cannot) be sensibly employed.

1. Introduction

In non-glaciated upland areas, bedrock rivers are the main geomorphic engines that transmit tectonic, climatic and lithological forcings into landscapes (e.g. Allen, 2008; Whipple et al., 2013). In doing so, these rivers not only incise bedrock but also transport sediment supplied to them (e.g. Whipple and Tucker, 2002; Finnegan et al., 2017). However, in most studies that invert channel morphology to map active deformation (e.g. Kirby et al., 2008), probe climatic variations (e.g. Leonard et al., 2023), and infer lithological controls (e.g. Gallen et al., 2013), channel dynamics are assumed to be dominated by incision (i.e. detachment-limited erosion). This assumption exploits the simplicity of the stream power law (SPL), in which incision is expressed as a function of drainage area and slope, both of which are readily available (Whipple and Tucker, 1999). Yet, this appealing assumption is likely flawed in most rivers that carry significant sediment (e.g. Whipple and Tucker, 2002). The expected importance of sediment supply at best complicates, and at worst may invalidate, the inferences drawn from prior studies using the SPL (Yanites, 2018). It is thus of fundamental importance to elucidate the extent to which sediment supply modulates long term channel dynamics in real rivers.

Sediments moving through channels have long been hypothesised to modulate incision and channel adjustment to tectonic forcing (Eq. (1), e.g. Sklar and Dietrich, 2006). If bedload sediment supply (Q_s) is low relative to channel transport capacity (Q_t), moving sediment tends to abrade and loosen bedrock to enhance incision (e.g. Sklar and Dietrich, 2004); in contrast, excessive relative sediment flux (Q_s/Q_t) covers the bedrock and inhibits incision (e.g. Johnson et al., 2009). This is often known as the "tools and cover" effect (Fig. 1), which has been examined in theoretical (e.g. Turowski et al., 2007), experimental (e.g. Sklar and Dietrich, 2001; Johnson and Whipple, 2010; Chatanantavet and Parker, 2008), modelling (e.g. Yamanishi and Naruse, 2026; Zhang et al., 2020), and some field perspectives (e.g. Cook et al., 2013; Jansen et al., 2011; Johnson et al., 2009). Yet, most field studies to date have focussed on the

* Corresponding author.
E-mail address: z.zhou22@imperial.ac.uk (Z. Zhou).

https://doi.org/10.1016/j.epsl.2026.120021
Received 30 July 2025; Received in revised form 14 January 2026; Accepted 27 March 2026

qualitative effects of sediment flux, leaving its quantitative function ($f(Q_s/Q_t)$) poorly constrained (Fig. 1). An important exception is Cowie et al. (2008), who supported a hump-shaped function for relative sediment flux in governing the erosional history of channels over timescales $>10^5$ years, based on well-constrained rivers crossing active faults in Italy and Greece. These authors ruled out an "undercapacity model" for governing long-term river incision (Beaumont et al., 1992), but their data did not resolve between published sediment flux functions that include tools and cover terms (Fig. 1, Sklar and Dietrich, 2004; Turowski et al., 2007).

To address this fundamental issue, we contrast two well-constrained rivers draining into the Gulf of Corinth, Greece. Both rivers cross marked gradients in bedrock erodibility and uplift rate (e.g. Zhou et al., 2024), and have good constraints on sediment supply (e.g. McLeod et al., 2024). We characterise the contrasting responses of the two rivers with distinct sediment fluxes to comparable tectonic and lithological gradients. In particular, the sensitivity of excess shear stress to tributary input is used to resolve competing relative sediment flux functions (c.f. Sklar and Dietrich, 2004; Turowski et al., 2007). In this context, we clarify the competing importance of channel slope versus width in reaching the excess shear stress required for equilibrium. The results give new insights into sediment flux-dependent river incision and help clarify when and why the SPL can be reasonably used for rivers carrying some or abundant sediment.

2. Flux-dependent incision

In general, flux-dependent incision can be modelled using Eq. (1):

$$E = Kf(Q_s / Q_T)(\tau_b - \tau_c)^a, \tag{1}$$

where E is incision rate, K is erodibility, $f(Q_s/Q_t)$ describes the "tools and cover" effect of relative sediment flux (i.e. Q_s/Q_t), τ_b is bankfull shear stress, τ_c is critical shear stress for incipient sediment motion, and a is a constant associated with the incision process (Hobley et al., 2011). The relative sediment flux function $f(Q_s/Q_t)$ can be interpreted as modulating the efficacy of excess shear stress (i.e. $\tau_b - \tau_c$) in incising bedrock (hereafter termed erosional efficacy, Johnson et al., 2009). Notably, the SPL ($E = KA^mS^n$, where A is drainage area, S is channel slope, and m and n are constants) can also be stated in terms of shear stress as $E = K(\tau_b - \tau_c)^a$ under common hydraulic scaling assumptions (Whipple and Tucker, 1999). In this sense, the SPL represents a special case of flux-dependent incision, in which $f(Q_s/Q_t)$ is a constant.

The relative sediment flux function is central to constraining river incision, but its specific form remains contentious (Fig. 1, e.g. Sklar and Dietrich, 2006). The basic form was first conceptualised (Sklar and Dietrich, 2004) and later validated by experimental studies (e.g. Johnson and Whipple, 2010) to depend on both sediment supply and the fraction of exposed bedrock (F_e). In Sklar and Dietrich (2004)'s conceptual model, the fraction of exposed bedrock is assumed to be linearly proportional to relative sediment flux (i.e. $F_e = 1 - Q_s/Q_t$), supported by flume experiments by Chatanantavet and Parker (2008). This results in a parabolic curve for $f(Q_s/Q_t)$ (Fig. 1), with the rising limb (tools domain) and falling limb (cover domain) being symmetrical with respect to the $Q_s/Q_t = 0.5$ axis (Eq. (2)).

$$f(Q_s / Q_t) = Q_s(1 - Q_s / Q_t), \tag{2}$$

Based on a probabilistic argument, however, Turowski et al. (2007) derived an exponential relationship between the fraction of exposed bedrock and relative sediment flux (i.e. $F_e = e^{-\varphi \frac{Q_s}{Q_t}}$, where φ represents the difference in the probability of excess sediment accumulation per unit bed area between exposed and covered areas). In this exponential relationship, the rate of decrease in the fraction of exposed bedrock diminishes as Q_s/Q_t increases. This leads to an asymmetrical $f(Q_s/Q_t)$ curve (Fig. 1), featuring a high-Q_s/Q_t range in which erosional efficacy becomes increasingly insensitive to Qs/Qt variations (Eq. (3)).

$$f(Q_s / Q_t) = Q_s e^{-\varphi \frac{Q_s}{Q_t}}, \tag{3}$$

This equation is derived for channels with $Q_s < Q_t$, in which all sediment is mobile, but dynamic cover can occur as sediment concentration increases, inhibiting the number of grain-bed collisions by increasing the frequency of grain-grain collisions (Turowski et al., 2007).

Even though experimental data can help constrain the form of $f(Q_s/Q_t)$ (Fig. 1; e.g. Sklar and Dietrich, 2004; Chatanantavet and Parker, 2008; Johnson and Whipple, 2010), their significance is limited

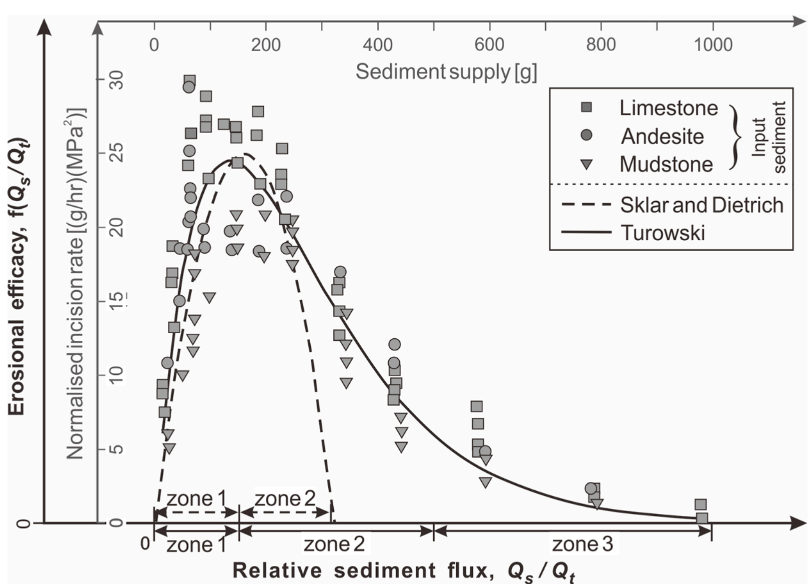

Fig. 1. Two competing, hump-shaped relative sediment flux functions—dashed (Sklar and Dietrich, 2004) and solid (Turowski et al., 2007)—are fitted to short-term experimental data from an erosion mill, in which sediments of different lithologies are input to abrade an underlying bedrock disk (scatters on grey axes; Sklar and Dietrich, 2001). Here, Turowski et al.'s (2007) function fits the scatters better than Sklar and Dietrich's (2004), but its significance is limited by differences in timescale and hydrodynamics between the experimental mill and natural rivers. Identifying the correct function is crucial, as the two predict distinct river dynamics (see main text). Note the Q_s/Q_t range can be conceptually divided into zones 1, 2, and 3, based on the gradient or sensitivity of the function to Q_s/Q_t variations.

by the extent to which the short-term erosion mill or flume experiments capture long-term river dynamics. To our knowledge, field evidence from natural rivers has yet to be found to resolve between the two formulations (e.g. Hobley et al., 2011). This is of fundamental importance, as the two functions predict distinct incision dynamics, partly due to differences in erosional efficacy gradients across the $Q_s\,/Q_t$ range. Up to three zones occur as a function of relative sediment flux: 1) a steep positive gradient (zone 1), 2) a steep negative gradient (zone 2), and 3) a shallow negative gradient (zone 3) (Fig. 1). Notably, zone 1 and zone 2 exist in both functions, but zone 3 is unique to Turowski et al.'s (2007) function, where the increasingly shallow gradient of the curve allows erosional efficacy to level off and therefore be effectively subsumed into erodibility K, whose dimensions are model-dependent (Eq. (1)). Thus, the existence of zone 3 in natural rivers may obscure the expected distinction between flux-dependent incision and the SPL (Whipple and Tucker, 1999). In addition, the two functions also differ in the Q_s/Q_t values at which zone 1 transitions into zone 2: this at 0.5 in Eq. (2) for Sklar and Dietrich (2004)'s formulation and at $1/\varphi$ in Eq. (3) for Turowski et al. (2007)'s. The value of φ is unknown, but the experiments suggest the transition occurs at $Q_s/Q_t \sim 0.2$, based on the assumption that incision ceases when $Q_s = Q_t$ (i.e. $Q_t = 1000$ g in Fig. 1). This transition point holds important implications for predicting incision rates in flux-dependent rivers (Turowski et al., 2007). In turn, the key distinctions described above provide the most effective means of

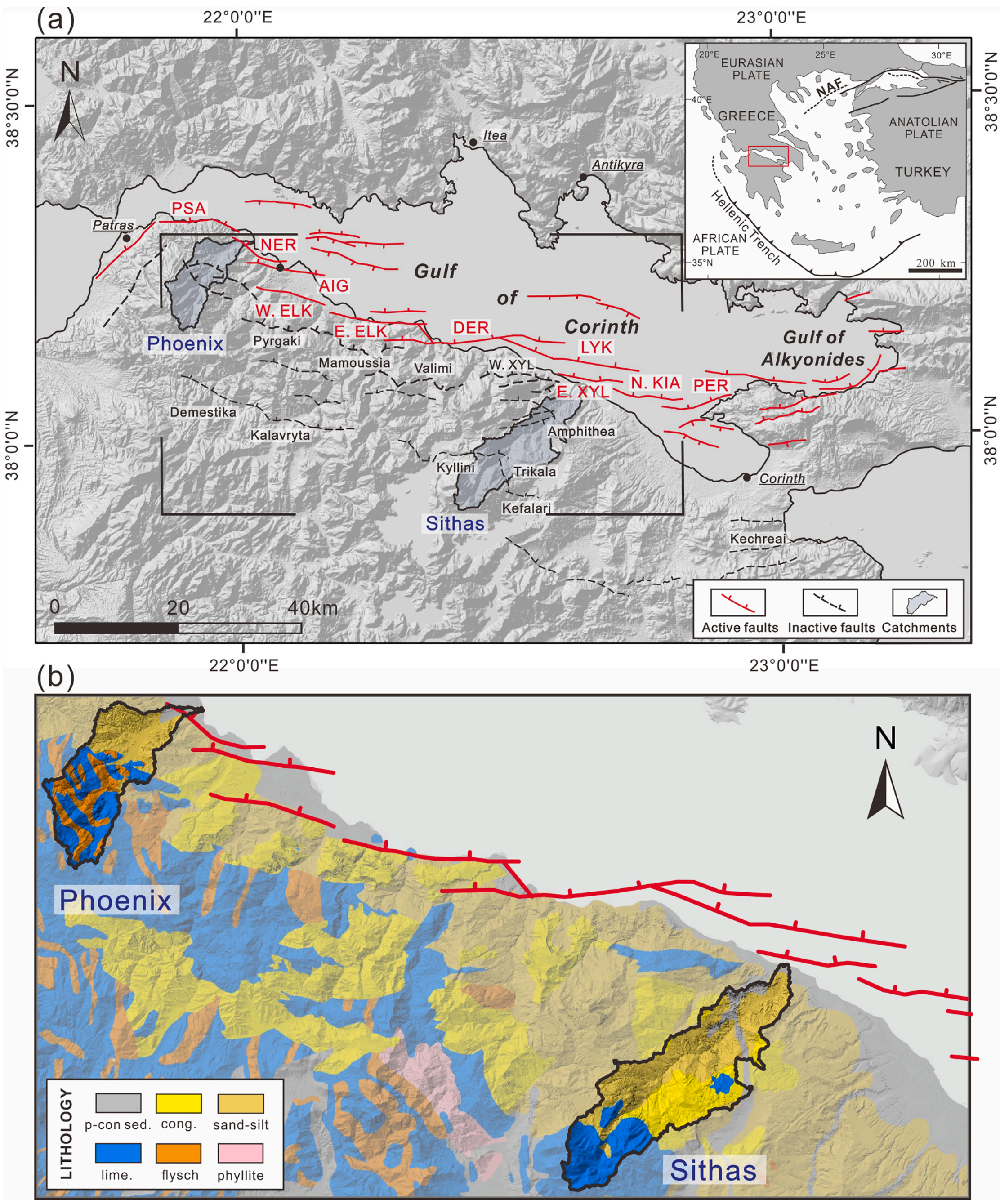

Fig. 2. Gulf of Corinth in maps of hillshaded relief (a), and lithology (b), with active faults (red lines) and the two study catchments highlighted. Abbreviations: p-con sed. – poorly consolidated sediment; cong. – conglomerate; sand-silt – sandstone-siltstone; lime. – limestone. AIG-Aigion fault, DER-Deveni fault, E. ELK-East Eliki fault, E. XYL-East Xylokastro fault, LYK-Lykoporia fault, N. KIA-North Kiato fault, PER-Perachora fault, PSA-Psathopyrgos fault, NER-Neo Erineos fault, W. ELK-West Eliki fault.

resolving the two competing functions (Fig. 1).

3. Study area

The Phoenix and Sithas are two rivers draining into the Gulf of Corinth, Greece, one of the fastest spreading active rifts in Europe (Fig. 2a; Bell et al., 2008). The Phoenix river crosses the onshore Selianitika and Erineos-Lampiri normal faults with a Late Quaternary footwall uplift rate of 1–2 mm/yr (Fig. 3c; Palyvos et al., 2010). The Sithas river is bounded by the offshore East Xylokastro fault, which has a comparable Late Quaternary uplift rate of 1.3–1.6 mm/yr (Fig. 3d; Armijo et al., 1996; de Gelder et al., 2019). The back-tilting of these fault blocks causes strike-perpendicular uplift rates to decline systematically, as evidenced by marine terraces (e.g. Armijo et al., 1996) and landscape characteristics (e.g. Fernández-Blanco et al., 2020). A linear decay model with a rate of ~0.08 $mmyr^{-1}km^{-1}$ broadly reproduces the strike-perpendicular uplift rate variations in Corinth (de Gelder et al., 2019; Zondervan et al., 2020).

Footwall rivers, such as the Phoenix and Sithas, experience a comparable downstream increase in uplift rate (Fig. 3c-d). The Phoenix river does not develop knickpoints in response to the onshore faults, but in the vicinity of the faults, the channel appears to have shifted toward alluvial conditions due to back-tilting (Fig. 3c). In contrast, the Sithas river is bounded by the older offshore fault and has developed two tectonic knickpoints (Fig. 3d, Zhou et al., 2024). Both rivers also traverse a similar bedrock erodibility gradient, from pre-rift basement upstream to syn-rift stratigraphy downstream (Fig. 2b, Zhou et al., 2024). The pre-rift basement, including limestone, flysch, and phyllites-quartzites (e.g. Wicker et al., 2024) is documented to be less erodible than the syn-rift stratigraphy comprising conglomerate, sandstone-siltstone, and poorly consolidated sediments (Fig. 2b, e.g. Zhou et al., 2024). In particular, limestone, flysch, and conglomerate, generate most of the bedload sediment, whereas sandstone–siltstone is rapidly abraded into sand-sized particles (Zhou et al., 2026).

Consequently, while Phoenix and Sithas rivers cross marked yet comparable gradients in bedrock erodibility and uplift rate (Fig. 3), both qualitative and quantitative observations indicate distinct bedload sediment supply. For example, Deiss et al. (2025) reported a 100-kyr bedload sediment budget for the Sithas of ~25 km^3/Myr, based on mapping of a deep-water fan offshore. This translates to ~2 kg/s using a mean sediment density of 2650 kg/m^3 and is several orders of magnitude lower than typical bankfull transport capacity (e.g. McLeod et al., 2024). As such, the Sithas river likely lies within the tools domain. Field observations show that during low-flow stages, coarse sediments only partially cover the Sithas channel (Fig. 3f), yet they fully mantle the Phoenix channel (Fig. 3e), suggesting considerable sediment supply in the latter catchment. This aligns with published findings that mass wasting, the main bedload generation process, is more pervasive in the Phoenix river than in the Sithas river (Fig. 3a-b, Zhou et al., 2026). In addition, based on seismic and field data, McLeod et al. (2024) estimated the Holocene bedload volume and bankfull sediment transport capacity for both rivers. Their results indicated that over the last 12 kyr, the *Qs/Qt* of the Phoenix river was ~2.5 times that of the Sithas river (their figure S6c), consistent with our qualitative field observations. In short, the two rivers exhibit distinct relative sediment fluxes, with the Sithas and Phoenix rivers likely falling in the tools and cover domains, respectively (Fig. 1).

The study rivers thus represent a unique opportunity to resolve between two competing relative sediment flux functions (Fig. 1). However, directly determining bankfull *Qs/Qt* downstream in rivers is non-trivial over long periods. This is because we typically lack hydrographs over 100-kyr timescales to constrain long-term bankfull flood intermittency and sediment transport capacity. Thus, we leverage variations in excess shear stress, and turn to the defining feature of zone 3, if present, i.e. its markedly lower sensitivity to *Qs/Qt* variations compared to the other two zones (Fig. 1) to reconstruct how these rivers are influenced by sediment flux dependent incision. In addition, available shorter-term *Qs/Qt* estimates introduced above are presented as corroborative

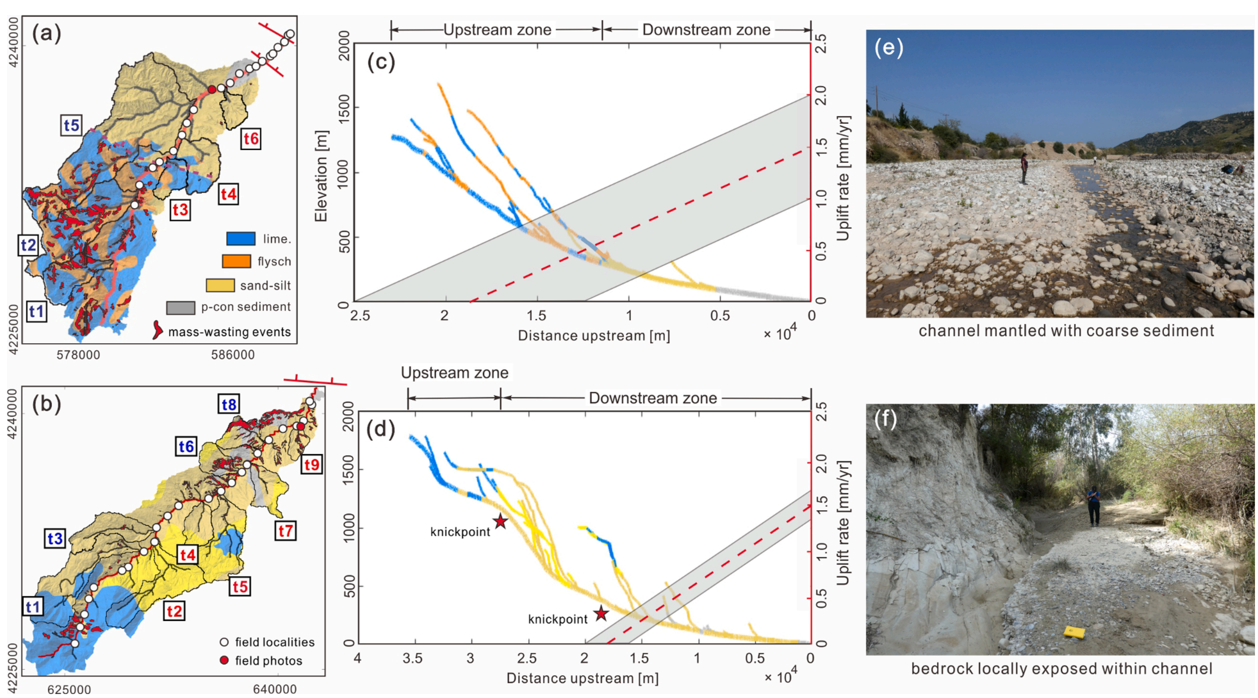

Fig. 3. Main characteristics of the Phoenix (a, c, e) and Sithas (b, d, f) rivers: (a, b) trunk and tributary channels cutting across different lithologies and normal faults; (c, d) trunk-channel river profiles, coloured by lithology from Fig. 2, shown with first-order variations in uplift rates. Dashed red lines and grey bands represent the mean and range of fault uplift rate constraints, with their upstream decrease based on the linear back-tilting model derived from two well-constrained faults in Corinth (see main text); (e, f) low-flow stage field observations (see locations in a and b). Note both rivers exhibit the transition between the upstream zone, where sediment input comes directly from adjacent coupled hillslopes, and the downstream zone, where tributary input dominates. The upstream-downstream transition coincides with the boundary between hard and soft bedrock in the Phoenix river and with a knickpoint in the Sithas river.

evidence.

4. Methods

To investigate sediment supply controls on river incision, we analysed channel morphological responses to variations in tectonics, lithology and sediment supply. For each river, we: i) systematically measured bankfull channel geometry; ii) evaluated excess shear stress responses to expected *Qs/Qt* variations across tributary confluences; and iii) constrained *Qs/Qt* values.

4.1. Bankfull channel geometry

Bankfull channel geometry, including width, slope, and depth, represents the main variable rivers adjust to accommodate variations in *Qs/Qt*, bedrock erodibility and uplift rates. These measurements are also essential to quantify excess shear stress and sediment transport capacities. In the field, we used flood markers, such as bleaching surfaces, vegetation boundaries, and debris to estimate bankfull stage (Fig. 4a, e.g. Whittaker et al., 2007). Then, channel width was measured as the distance between the bounding channel banks (Fig. 4b) using a laser rangefinder. Slope was determined in degrees over ~30 m along the river (Fig. 4c). Depth was measured as the elevation differences from thalweg points to flood markers (Fig. 4d). Errors associated with these measurements are provided in supplementary methods.

To characterise channel responses to marked variations in lithology and tectonics, bankfull width, slope, and wdith: depth (*W/D*) were plotted along the trunk channel in both rivers (Fig. 5a-d). Because channel width and slope scale with drainage area, area-normalised slope (steepness, k_{sn}) (Eq. (4)) and width (wideness, k_{wn}) (Eq. (5)) were introduced to account for area-induced variations:

$$k_{sn} = SA^{b}, \tag{4}$$

$$k_{wn} = WA^{-c}, \tag{5}$$

where S is the channel slope, A is the upstream drainage area, W is the channel width, b and c are exponents relating drainage area to slope and width, respectively (e.g. Allen et al., 2013). In our calculations, b and c were set as 0.5 for both rivers to enable direct comparison (e.g. Yanites, 2018), with uncertainties propagated. In this study, we compared the relative variability of wideness and steepness to infer the dominant mechanism (width versus slope adjustment) a river uses to accommodate gradients in bedrock erodibility and uplift rate: slope adjustment prevails if steepness is more variable; alternatively, width adjustment dominates.

4.2. Excess shear stress and tributary input

To test the hypothesis that the sediment-rich Phoenix river may lie in zone 3 (Fig. 1), the sensitivity of erosional efficacy to *Qs/Qt* variations was examined. Erosional efficacy cannot be measured directly, but for channels that are in erosional equilibrium with identical uplift rates and erodibility, it is inversely related to excess shear stress (Eq. (1)). Thus, in such channel reaches, the objective can be reframed as examining the sensitivity of excess shear stress to *Qs/Qt* variations. Excess shear stress was calculated here as bankfull shear stress minus critical shear stress, both of which can be derived directly from our bankfull channel geometry measurements (supplementary methods).

In both rivers, the downstream zones are point-sourced by tributary inputs (Fig. 3; Zhou et al., 2026), making tributary confluences an ideal

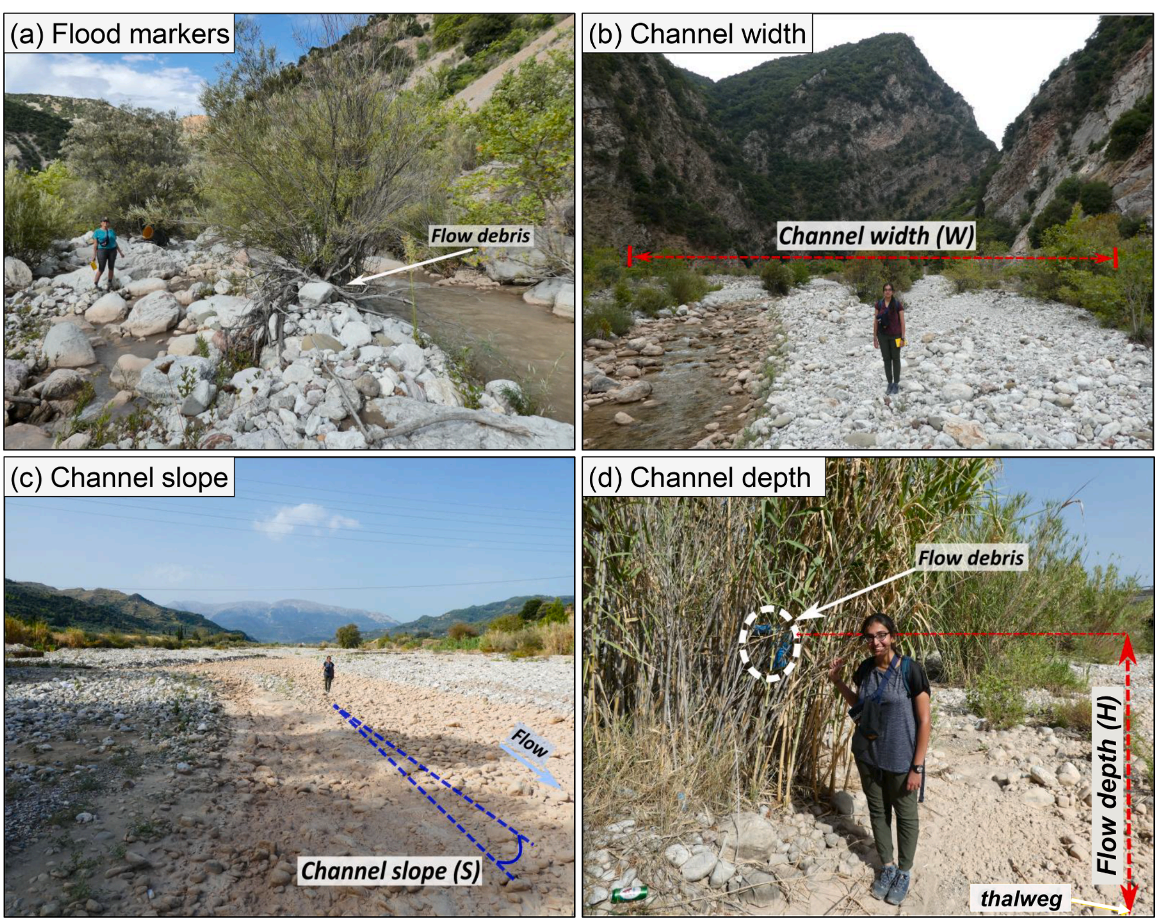

Fig. 4. Field photos illustrating bankfull flood markers (A), width (B), slope (C), and depth (D).

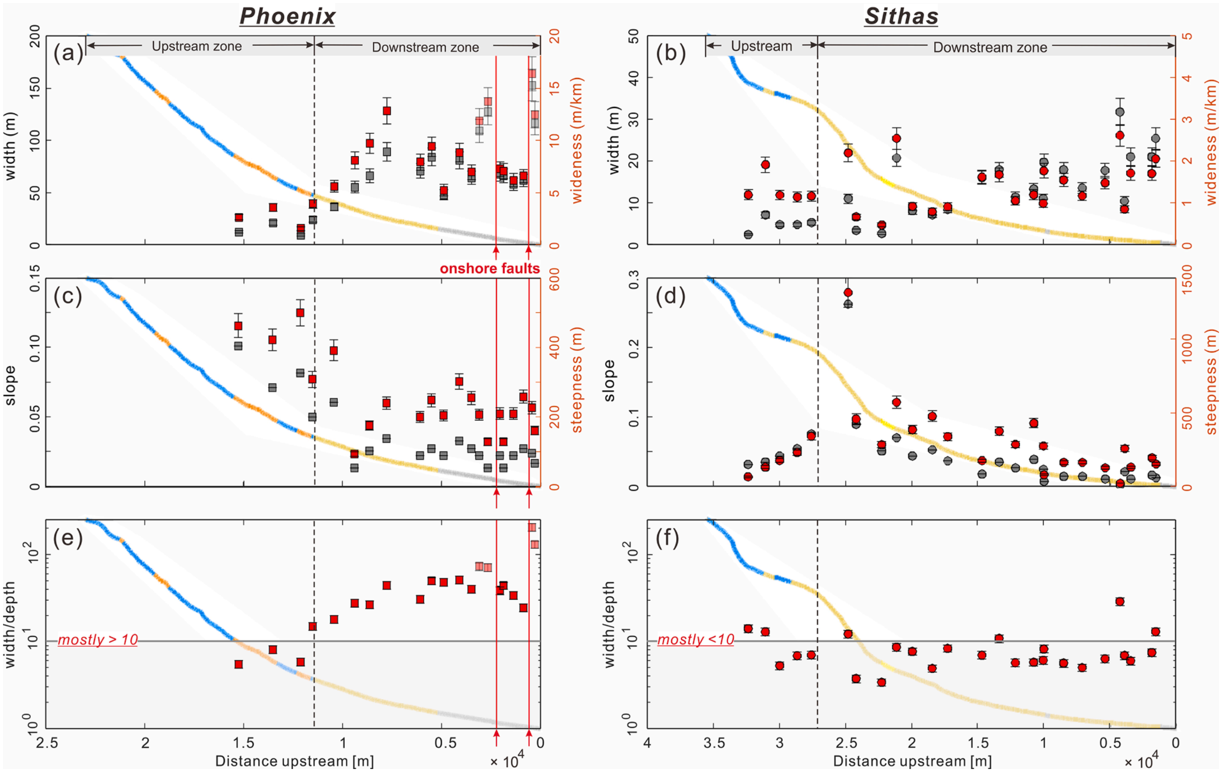

Fig. 5. Bankfull width (grey) / wideness (red) (a, b), slope (grey) / steepness (red) (c, d), and width:depth, *W/D* (e, f) along the lithology-coloured trunk-channel river profiles for the Phoenix (a, c, e) and Sithas (b, d, f) rivers. Note the Phoenix river is dominated by width adjustments, whereas the Sithas river is dominated by slope adjustments. The onshore faults (Fig. 3a) are marked as red lines, and the four transparent markers in the Phoenix river represent channels interpreted to be close to transport-limited alluvial conditions (see main text for details). See Fig. 3 for lithology legend.

context for investigation. This is because the trunk channel *Qs/Qt* may change markedly across confluences due to tributary sediment input, while uplift rates and lithology remain effectively constant over such short distances. Between confluences, uplift rates are expected to increase towards the faults, but we make the simplifying assumption that *Qs/Qt* is approximately spatially uniform as sediment and water discharge is not expected to change. From the perspective of sediment mixing, the impact of tributary input on the trunk channel's *Qs/Qt* depends mostly on their differences in *Qs/Qt* and drainage area. The latter is readily available, but the former is hard to constrain directly. Here, we leveraged the published finding that bedload sediment in our study rivers is dominantly generated from limestone, flysch, and conglomerate, as the softer sandstone–siltstone is documented to be rapidly abraded into sand-sized particles and therefore does not contribute to bedload (Zhou et al., 2026). This allows us to use the combined area of limestone, flysch, and conglomerate, relative to the total drainage area (bedload-generating-lithology proportion), as a qualitative proxy for relative sediment flux. Note, this proxy is not used here to quantify *Qs/Qt* along the trunk channels; rather, it is used in conjunction with drainage area to assess which tributaries are most or least likely to change the trunk-channel *Qs/Qt* at confluences. Specifically, tributaries with distinct bedload-generating-lithology proportions and large drainage areas relative to the trunk-channel are most likely to change the trunk-channel *Qs/Qt* at confluences (supplementary Table S2).

Consequently, we plotted excess shear stress (supplementary methods) along the trunk-channel profiles for both rivers, with the positions of tributary confluences shown (Fig. 6). First, we examined excess shear stress variations between confluences to test whether the surveyed channels are in equilibrium with the gradients in uplift rate and erodibility. In this context, we then compared the magnitude of excess shear stress variations with that of the expected *Qs/Qt* changes (supplementary Table S2) across confluences to assess the sensitivity of excess shear stress to *Qs/Qt* changes: if a tributary expected to significantly disturb the trunk-channel *Qs/Qt* does not alter excess shear stress, the erosional efficacy of the river is considered insensitive to *Qs/Qt* variations (zone 3). In contrast, if a tributary assessed to have limited impact on the trunk-channel *Qs/Qt* corresponds to a marked change in excess shear stress, the erosional efficacy of the river is considered highly sensitive to *Qs/Qt* variations (zone 1 or zone 2).

4.3. *Qs/Qt* estimates

The interpretation drawn from the sensitivity analysis can be complemented by our independent constraints on bankfull *Qs/Qt* values of the two rivers. We exploited the observation that the Phoenix river appears to transition to dominantly alluvial conditions near the onshore active faults (Zhou et al., 2026). In transport-limited alluvial reaches, excess shear stress is, by definition, all spent to transport sediment (i.e. $Qs = Qt$), and transport capacity can be estimated using the Meyer-Peter and Müller equation (supplementary methods). Thus, we estimated maximum *Qs* from the dominantly alluvial channels (transparent points in Fig. 5a, c, e) and *Qt* from channels adjacent to those dominantly alluvial ones (supplementary methods and Table S1). The *Qs/Qt* can be therefore constrained for the Phoenix river and then extrapolated to the Sithas river, based on its ~2.5-fold difference over the last 12 kyr (McLeod et al., 2024) and the likely equal number of bankfull floods in the two adjacent rivers.

5. Results

5.1. Bankfull channel geometry

Fig. 5 shows downstream variations in bankfull width, slope, and *W/D*, as the Phoenix and the Sithas rivers traverse comparable gradients in

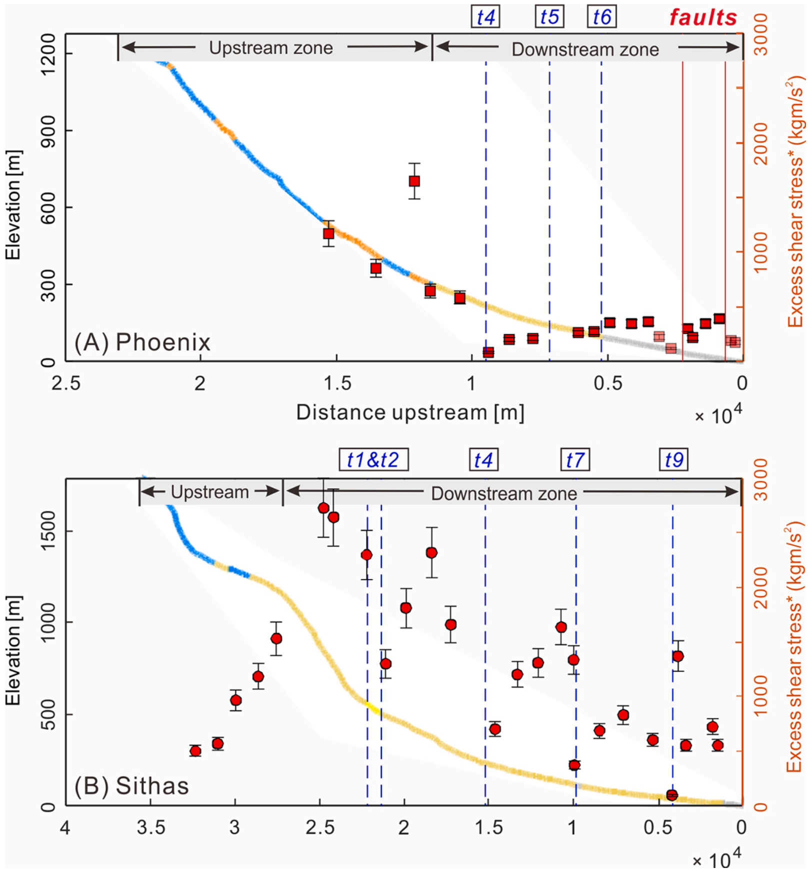

Fig. 6. Downstream variations in excess shear stress along the lithology-coloured trunk-channel river profiles for the Phoenix (a) and Sithas (b) rivers, with the locations of tributary confluences marked (dashed blue lines). Note the sensitivity of excess shear stress to tributary input differs significantly between the Phoenix and Sithas rivers. The four transparent markers in the Phoenix river represent channels interpreted to be close to transport-limited alluvial conditions (see main text for details). See Fig. 4 for lithology legend.

bedrock erodibility and uplift rate (Fig. 3) with distinct sediment fluxes. In the sediment-rich Phoenix river, channels first widen markedly from the hard-bedrock dominated upstream zone (~15 m) to the soft-bedrock dominated downstream zone (~90 m), and then narrow towards active faults, where uplift rates increase (Fig. 5a). This narrowing fails to manifest just upstream or downstream of the faults, where the four widest channels in the river are located (~120 m) (Fig. 5a). This is interpreted as a shift in their channel dynamics toward dominantly alluvial conditions due to fault back-tilting (e.g. Humphrey and Konrad, 2000). Notably, the dramatic variations in width (~10–150 m) persist even after normalisation by drainage area (i.e. wideness ~1.5–16 m/km) (Fig. 5a). In comparison to width, across the same gradients in bedrock erodibility and uplift rate, channel slope exhibits less variation (~0.014–0.1), most of which occurs in the hard-bedrock-dominated upstream zone (Fig. 5c). This pattern is also clear in steepness, where the upstream channel k_{sn} fluctuates between ~300–500 m while the downstream channels stabilise at ~210 m (Fig. 5c). The relative variability of wideness and steepness suggests that, except in the upstream zone, width adjustment is the main mechanism the sediment-rich Phoenix river uses to accommodate variations in bedrock erodibility and uplift rate. W/D is mostly <10 in the upstream zone and increases to ~50 in the downstream zone, with the dominantly alluvial reaches reaching ratios up to 110 (Fig. 5e).

In contrast, for the sediment-poor Sithas river, channel width increases gradually from 2 m to 25 m downstream (Fig. 5b). Yet, most of the width increase can be explained by drainage area, given only limited variation remains in wideness (0.5–2.5 m/km) (Fig. 5b). Compared to width, channel slope increases from 0.03 to 0.25 near the knickpoint and then decreases downstream to 0.01 (Fig. 5d). These variations persist in steepness, even when the impact of drainage area is accounted for (~20–1300 m, Fig. 5d). The much larger relative variability in slope compared to width suggests that slope adjustment is the main mechanism by which the sediment-poor Sithas river tries to achieve equilibrium. W/D is <10 across most channels, with no clear pattern observed (Fig. 5f).

Taken together, the two rivers, with distinct sediment fluxes, differ in their morphological responses to comparable gradients in bedrock erodibility and uplift rate: the sediment-rich Phoenix mostly adjusts width, except in its upstream zone; in contrast, the sediment-poor Sithas predominantly adjusts slope (Fig. 5a-d). In both rivers, the slope-dominated channel response appears to occur when W/D is approximately less than 10. This contrast in morphological response points to the crucial role of sediment supply in shaping the channel geometry.

5.2. Downstream variations in excess shear stress

Fig. 6 plots excess shear stress along the trunk of the Phoenix and Sithas rivers, with tributary confluences marked as dashed blue lines. In the sediment-rich Phoenix, excess shear stress is ~3 times higher upstream than in the downstream zone (Fig. 6a). This aligns with estimated variations in bedrock erodibility (Zhou et al., 2024), supporting the idea that the river has equilibrated with changing bedrock erodibility. In the downstream zone, excess shear stress increases almost linearly towards the faults (Fig. 6a), consistent with the variations in uplift rates (Fig. 3c). Notably, excess shear stress does not deviate significantly downstream of tributary confluences, where Qs/Qt is expected to change (Fig. 6a). For example, tributary t5 has a bedload-generating-lithology proportion of 45% and a drainage area of 27 km^2, both of which are significant relative to those of the trunk channel (86%, 48 km^2, respectively in supplementary Table S2). Its confluence with the trunk channel is expected to markedly disturb the trunk *Qs/Qt*, yet excess shear stress exhibits little corresponding response (Fig. 6a). This implies that erosional efficacy remains approximately constant despite variations in *Qs/Qt* due to tributary input. This could occur either if the river approaches detachment-limited conditions or if the river lies in zone 3, where erosional efficacy is insensitive to *Qs/Qt* variations (Fig. 1); however, the former can be excluded based on the clear observation that the channel is covered by coarse sediment (Fig. 3e). Consequently, we interpret that the sediment-rich Phoenix river lies in zone 3.

In the sediment-poor Sithas river, excess shear stress shows a general downstream increase within reaches between tributary confluences, where *Qs/Qt* is approximately constant (Fig. 6b). This is consistent with the trend in uplift rates (Fig. 3d), supporting the notion that the channels are in equilibrium. Yet, when sediment-rich tributaries known to coarsen trunk-channel sediment grain size join the trunk channel, such as t2, t4, and t7, excess shear stress decreases markedly (Fig. 6b) (c.f. Zhou et al., 2026). Because these channels are in equilibrium, the reduction in excess shear stress must have been compensated by a corresponding increase in erosional efficacy across these tributary confluences (e.g. Cowie et al., 2008). Tributary t7, with a bedload-lithology proportion of 29% but a small drainage area of 6 km^2 relative to the trunk channel (52%, 125 km^2, respectively in Table S2), is expected to have limited impact on trunk-channel's *Qs/Qt*; however, excess shear stress drops to one-third of its initial value downstream of the confluence (Fig. 6b). This observation suggests that excess shear stress and, therefore erosional efficacy, is highly sensitive to *Qs/Qt* variations. Thus, we interpret that the sediment-poor Sithas river lies in zone 1 (Fig. 1).

5.3. Constraints from Qs/Qt estimates

To further assess the interpretation of the *Qs/Qt* zones in which the two rivers fall, the *Qs/Qt* values are approximated. In the Phoenix river, bankfull *Qs* can be estimated from dominantly transport-limited reaches at $\sim$6000 kg/s, and bankfull *Qt*, estimated from adjacent flux-dependent reaches, is $\sim$7700 kg/s (see supplementary methods and Table S1 for details). The Phoenix river's *Qs/Qt* is therefore constrained at $\sim$0.8, aligning with its interpreted position in zone 3 (Fig. 1). Combined with the finding that the *Qs/Qt* of the Phoenix river is $\sim$2.5 times that of the Sithas river (McLeod et al., 2024), our constraint on the Phoenix river can be extrapolated to the Sithas river (*Qs/Qt* $\sim$ 0.3). This is consistent with its interpreted position in the tools domain (zone 1) (Fig. 1).

6. Discussion

6.1. Constraints on the relative sediment flux function

We show two rivers with distinct sediment fluxes exhibit contrasting morphological responses to comparable gradients in bedrock erodibility and uplift rates (Fig. 5). This is inconsistent with predictions from the SPL for detachment-limited rivers (e.g. Finnegan et al., 2005) but aligns with the effects of flux-dependent dynamics (e.g. Yanites and Tucker, 2010). In both rivers, excess shear stress variations across tributary confluences (Fig. 6) are interpreted to reveal the sensitivity of erosional efficacy to *Qs/Qt* variations, with the sediment-rich Phoenix River being much less sensitive than the sediment-poor Sithas River. In particular, the sediment-rich Phoenix river is estimated to have a *Qs/Qt* of $\sim$ 0.8.

The high *Qs/Qt* zone (with markedly decreased sensitivity to *Qs/Qt* variations) is absent from Sklar and Dietrich's (2004) function but is integral to Turowski et al. 's (2007) function (zone 3 in Fig. 1). Essentially, the existence of zone 3 is a direct result of the diminishing rate of decrease in the fraction of exposed bedrock as *Qs/Qt* increases. This feature, however, is challenging to discern directly in experimental studies (Johnson and Whipple, 2010). Hobley et al. (2011) found their optimal sediment flux functions for three rivers flowing over coarse and loose postglacial debris are comparable in form to Turowski et al. 's (2007) function. Yet, this study is interpreted to provide ambiguous support for Turowski et al. 's (2007) function as the rivers they document never incise into bedrock and could therefore be transport-limited (Hobley et al., 2011). Thus, to our knowledge, our evidence for a zone 3 river (i.e. the Phoenix river) represents the first unambiguous field support for Turowski et al.'s (2007) function over Sklar and Dietrich's (2004) for relative sediment flux (Fig. 1).

The decreased sensitivity of erosional efficacy to *Qs/Qt* variations at high *Qs/Qt* values (Turowski et al., 2007) helps reconcile some long-standing conflicting observations. Below, we focus on the elusive role of width versus slope in channel response to external forcings, the mixed success of the SPL, and the implications for interpreting flux-dependent river incision.

6.2. Channels increase shear stress: to steepen or to narrow?

In principle, rivers can narrow or steepen to increase shear stress (Equation S2), but how this adjustment is partitioned between changes in width and slope remains elusive (e.g. Yanites and Tucker, 2010). It has been explored in numerical models incorporating flux-dependent incision, but such models often use overly simplified relative sediment flux functions or assume that channels reach their steady-state width at which slope is minimised (Turowski et al., 2009; Yanites and Tucker, 2010). Moreover, rivers with well-constrained sediment fluxes have been scarce for model validation. Here, we take the opportunity to explore what our results may imply about the contrasting dynamics of narrowing compared to steepening in sediment-influenced bedrock rivers.

In our study, the sediment-poor Sithas river has a *W/D* mostly $<$10 (Fig. 5f). This *W/D* is close to a threshold value, below which shear stress maxima shift from the channel centre to the banks due to increased friction near the banks (e.g. Turowski et al., 2008). This mechanism, first examined in detachment-limited conditions, has been invoked to limit channel narrowing (e.g. Wobus et al., 2006). This is because further narrowing results in shear stress on the banks exceeding that on the bed, which increases bank incision and counteracts the narrowing. In contrast, channel slope—affecting only the magnitude, rather than the cross-sectional distribution, of shear stress—is still free to adjust. Consequently, rivers at a threshold width mostly steepen, rather than narrow, to increase their erosive power (e.g. Wobus et al., 2006). The same pattern is observed in the Sithas river (Fig. 5b, d), in the zone 1 tools domain (Fig. 6b), in which erosional efficacy increases as sediment concentration increases. This motivates us to propose how the threshold width model may be extended to flux-dependent rivers: when the channel bed and banks share limited sediment, sediments are expected to concentrate in areas of higher shear stress (e.g. Meyer-Peter and Müller, 1948), meaning the erosional efficacy of the bed and banks is shear-stress dependent. Incision in such flux-dependent channels thus depends only on shear stress, similar to the SPL (Eq. (1)), and channel cross-section equilibrium is consequently reached at the threshold width, where shear stress between the bed and banks is balanced: any further narrowing or widening is counteracted by subsequent redistribution of shear stress (Fig. 7a).

Unlike the Sithas river, the sediment-rich Phoenix river in its downstream zone is significantly wider than a threshold width (Fig. 5e), as observed in other studies (e.g. Baynes et al., 2020; Finnegan et al., 2017). In channels wider than the threshold width, shear stress is expected to be much higher on the bed than on the banks (e.g. Turowski et al., 2008). The Phoenix river as a whole is interpreted to lie in zone 3, so the channel bed with higher shear stress must also be in zone 3, as sediment concentration depends on shear stress (e.g. Meyer-Peter and Müller, 1948). The banks with lower shear stress should have lower sediment concentration and therefore higher erosional efficacy, likely zone 2 for the banks of the Phoenix river (Fig. 7b). This may explain why sediment-rich rivers, such as the Phoenix river, are wider than

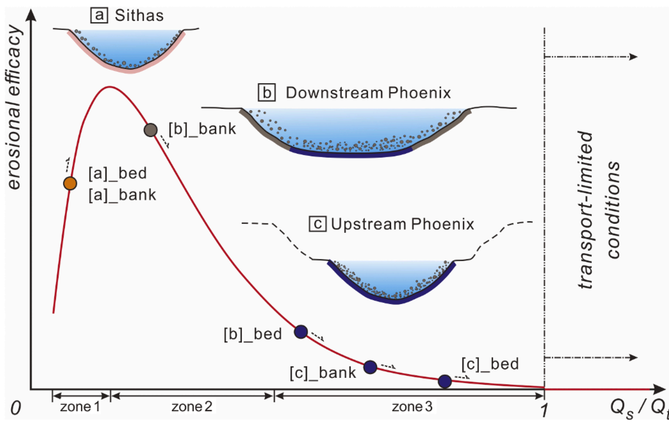

Fig. 7. A schematic diagram illustrating the 'tools and cover' effect of sediment in shaping channel equilibrium geometry. Note, channels a and c exhibit similar channel geometry despite significant differences in relative sediment flux, because both have limited contrast in erosional efficacy between the channel bed and banks. Furthermore, this contrast does not change significantly when there is an increase in *Qs/Qt*, as indicated by dash arrows. In contrast, channel b, where the bank efficacy exceeds bed efficacy, exhibits a much wider channel. The increasingly shallow gradient of the curve in the cover domain causes a *Qs/Qt* increase to reduce bank efficacy more than bed efficacy, as indicated by dash arrows.

sediment-poor rivers (e.g. the Sithas river): shear stress on the bed must be high enough to compensate for its lower efficacy (Fig. 7b).

Importantly, channels in this condition are free to narrow or steepen to increase erosive power. In the downstream Phoenix river, however, the channels mostly adjust width, rather than slope, to accommodate variations in bedrock erodibility and uplift rate (Fig. 5a,c). Similar observations have also been reported in both ancient (Amos and Burbank, 2007) and modern (Yanites et al., 2010; Allen et al., 2013) sediment-rich rivers. This raises the question: why does a wide channel mostly adjust width to modulate its erosive power? Here, we hypothesise that, for channels such as the downstream-most reach of the Phoenix river, steepening alone can, in theory, elevate erosive power to balance increasing uplift rates towards the fault, but such steepened channels are not in full equilibrium: any perturbations that increase sediment concentrations can trigger an incision imbalance across the channel cross-section. This is because, for a given increase in *Qs/Qt*, bank efficacy in zone 2 decreases more strongly than bed efficacy in zone 3, due to the increasingly shallow gradient of the f(*Qs/Qt*) in Turowski et al. 's (2007) formulation (Fig. 7c). In this case, bank incision is surpassed by bed incision, promoting narrowing that increases sediment concentrations further (Fig. 7c). This positive feedback loop continues until the channel narrows to a width where bank incision catches up with bed incision (Eq. (1)), and a new equilibrium is reached. In this process, the initial steepening is partly or fully erased as channels maintain equilibrium with the imposed uplift rates. Thus, wide channels would preferentially adjust their width to increase erosive power. If channels are narrowed to near their threshold width, however, further narrowing is inhibited and steepening becomes important again, as in the upstream Phoenix and other sediment-rich rivers (e.g. Amos and Burbank, 2007; Yanites et al., 2010; Allen et al., 2013). Here, we propose that in such channels, both the bed and banks have entered zone 3, where their difference in erosional efficacy approaches zero (Fig. 7c). This again causes incision to depend mostly on shear stress, similar to the SPL (Eq. (1)). As a result, any narrowing can be counteracted by the subsequent increase in shear stress on the bed relative to the banks (Fig. 7c).

Thus, a conceptual channel geometry model that is built upon the constrained flux-dependent incision and the equilibrium principle is proposed (Fig. 7; c.f. Yanites and Tucker, 2010; Turowski et al., 2007). The model predicts the relative sediment flux conditions under which width or slope dominates channel morphological adjustments to changing boundary forcing (c.f. Yanites and Tucker, 2010; Yanites, 2018). In this model, sediment-rich rivers can be as narrow as bedrock rivers, a somewhat counterintuitive observation recently derived from ~1300 well-documented channels (Buckley et al., 2024). However, testing and validating this conceptual model requires more field, numerical, and experimental work that compares channel width and slope responses to known forcing.

6.3. Implications of flux-dependent incision for river interpretation

In general, our results illustrate that moving sediment exerts a dual control on channel geometry: first, by determining the excess shear stress required to maintain equilibrium with boundary conditions (Fig. 6), and second, by influencing how that shear stress is partitioned between width and slope adjustments (Fig. 7). This recognition consolidates the theoretical importance of sediment supply and raises questions about the applicability of the SPL (Yanites, 2018). Yet, it works surprisingly well in many rivers, even in sediment-rich ones (e.g. Lavé and Avouac, 2001; Yanites et al., 2010). Thus, we consider when and why the SPL can be reasonably used in river interpretation.

The SPL can be considered as a upscaled version of Eq. (1), when erosional efficacy is constant and channel width scales only exponentially with drainage area (e.g. Whipple and Tucker, 1999). Its application therefore hinges on the extent to which these two conditions are met. For rivers with some sediment, such as the Phoenix river, their erosional efficacy is highly sensitive to variations in *Qs/Qt* (zone 1 in Fig. 1). Here, maintaining equilibrium requires that excess shear stress and, implicitly, bankfull channel geometry must adjust significantly in response to variations in *Qs/Qt*. Furthermore, the excess shear stress in such rivers is adjusted mostly by slope, rather than width changes (Fig.7a), allowing the SPL to be effective at a reach scale where *Qs/Qt* is constant, but not across confluences where *Qs/Qt* might change (e.g. Zhou et al., 2024). In rivers carrying abundant sediment (e.g. the Phoenix river), however, channels may enter zone 3 of Turowski et al. (2007)'s function in which erosional efficacy becomes insensitive to changes in *Qs/Qt* (Fig. 1). In this case, *Qs/Qt* variations are not the limiting condition as erosional efficacy is nearly constant; instead, the critical constraint is channel-width dynamics. If the banks are yet to reach zone 3, width changes are the preferred mechanism to adjust shear stress (e.g. the downstream Phoenix; Fig. 7b). As a result, the SPL cannot be used to indicate incision rates across the whole river, but other shear-stress based incision laws that explicitly incorporates channel width can be used (e.g. Lavé and Avouac, 2001; Yanites et al., 2010). Once the banks also lie within zone 3, channel morphological adjustments are again mostly manifested as slope changes (e.g. the upstream Phoenix; Fig.7c). In such rivers, the SPL can capture the main characteristics of flux-dependent rivers.

Our results explain the mixed success of the SPL when tested against independent field evidence. For example, only in channels dominated by slope adjustments are channel steepness (i.e. drainage area-normalised slope) and knickpoints likely to be effective in mapping active deformation. In addition, the linear correlation between incision rate and excess shear stress in both the Phoenix and other zone 3 rivers (e.g. Lavé and Avouac, 2001; Yanites et al., 2010) suggest that the commonly observed nonlinearity in the incision rate – steepness relationship might arise from i) the inappropriate use of steepness in rivers dominated by width adjustments, and ii) variations in *Qs/Qt*. These insights are important because the SPL, due to its simplicity, has been, and will likely continue to be, a "default" model for river incision. Our approach helps to assess the confidence we should place in previous studies that used the SPL, and to choose appropriate rivers for its future use.

Taking flux-dependent dynamics fully into account is impeded by the lack of quantitative constraints on *Qs/Qt*; however, its impact on river incision interpretation can be minimised. A critical step in this effort is to identify the *Qs/Qt* zone of the study rivers (cf. Fig. 1). This can be achieved by analysing *W/D* and the sensitivity of excess shear stress to tributary input. As discussed in Section 6.2, rivers with *W/D* approaching ~10 are likely to lie either within zone 1 or zone 3, with the latter further distinguished by insensitivity of excess shear stress to tributary input. The *Qs/Qt* range of the rivers can then be used to guide further analysis. For example, relationships between tectonics, lithology, and topography should be examined in zone 3 rivers. In addition, excess shear stress serves as a recommended proxy for external forcing, especially in zone 2 rivers.

7. Conclusions

This study shows that two rivers, with distinct sediment fluxes, exhibit contrasting morphological responses to comparable tectonic and lithological gradients. In the sediment-poor Sithas river, excess shear stress is sensitive to tributary input, consistent with the tools effect of sediment supply (zone 1 in Fig. 1). In contrast, in the sediment-rich Phoenix river, with a *Qs/Qt* of ~0.8, excess shear stress exhibits little response to tributary input. This supports the existence of a high *Qs/Qt* zone, in which erosional efficacy approaches a constant (zone 3 in Fig. 1). This behaviour is absent from Sklar and Dietrich's (2004) tools versus cover effect model of sediment flux dependent incision but is an integral part of the Turowski et al. 's (2007) model, in which the rate of decrease in the exposed bedrock fraction diminishes as *Qs/Qt* increases. This, to our knowledge, represents the first unambiguous field evidence favouring Turowski et al. 's (2007) function and suggests that the erosional efficacy of rivers is best described by an asymmetric sediment flux function that incorporates tools and cover effects.

In reaching the excess shear stress required to maintain equilibrium, the sediment-poor Sithas river mostly adjusts its slope, whereas the sediment-rich Phoenix river mostly adjusts its width, except in its upstream sections. Importantly, the changing importance of slope versus width can be explained by flux-dependent behaviour in channels that follow Turowski's relative sediment flux equation. Consequently, we conclude that sediment controls channel geometry not only by determining the excess shear stress required to balance boundary conditions, but also by influencing how that excess shear stress is partitioned between width and slope adjustments.

The stream power law is a special case of sediment flux-dependent incision, and we argue it is most effective where *Qs/Qt* is relatively constant down-system or where the river lies in the high *Qs/Qt* zone characterised here (zone 3 in Fig. 1), in which additional sediment flux does not significantly change erosional efficacy. In addition, the finding that channel response to external forcing is sediment flux-dependent challenges common tectonic interpretations of long profiles because some rivers mostly adjust width, rather than slope, in response to forcing such as active faulting. To minimise the impact of flux-dependent dynamics, we advocate examining the *Qs/Qt* zone of rivers as a routine part of fluvial geomorphology.

CRediT authorship contribution statement

Ziqiang Zhou: Writing – original draft, Visualization, Methodology, Investigation, Funding acquisition, Formal analysis, Conceptualization. **Reha Chandresh:** Writing – review & editing, Visualization, Methodology, Investigation, Formal analysis. **Alexander C. Whittaker:** Writing – review & editing, Supervision, Methodology, Investigation, Funding acquisition, Conceptualization. **Gary J. Hampson:** Writing – review & editing, Supervision, Conceptualization. **Rebecca E. Bell:** Writing – review & editing, Supervision, Investigation.

Declaration of competing interest

The authors declare that they have no known competing financial interests or personal relationships that could have appeared to influence the work reported in this paper.

Acknowledgement

ZZ was supported by an Imperial College Janet Watson Studentship and RC was supported by Imperial College London. We thank the two anonymous reviewers for their constructive comments, which greatly improved the clarity of the work.

Supplementary materials

Supplementary material associated with this article can be found, in the online version, at doi:10.1016/j.epsl.2026.120021.

Data availability

The authors confirm that all data required to reproduce the key findings of this paper are provided within the manuscript or its supplementary materials.

References

Allen, G.H., Barnes, J.B., Pavelsky, T.M., Kirby, E., 2013. Lithologic and tectonic controls on bedrock channel form at the northwest Himalayan front. J. Geophys. Res. Earth Surf. 118, 1806–1825. https://doi.org/10.1002/jgrf.20113.
Allen, P.A., 2008. From landscapes into geological history. Nature 451, 274–276. https://doi.org/10.1038/nature06586.
Amos, C.B., Burbank, D.W., 2007. Channel width response to differential uplift. J. Geophys. Res. 112. https://doi.org/10.1029/2006JF000672, 2006JF000672.
Armijo, R., Meyer, B., King, G.C.P., Rigo, A., Papanastassiou, D., 1996. Quaternary evolution of the Corinth Rift and its implications for the late cenozoic evolution of the Aegean. Geophys. J. Int. 126, 11–53. https://doi.org/10.1111/j.1365-246X.1996.tb05264.x.
Baynes, E.R.C., Lague, D., Steer, P., Bonnet, S., Illien, L., 2020. Sediment flux-driven channel geometry adjustment of bedrock and mixed gravel–bedrock rivers. Earth Surf. Process. Landf. 45, 3714–3731. https://doi.org/10.1002/esp.4996.
Beaumont, C., Fullsack, P., Hamilton, J., 1992. Erosional control of active compressional orogens. In: McClay, K.R. (Ed.), Thrust Tectonics. Chapman & Hall, New York, pp. 1–18.
Bell, R.E., McNeill, L.C., Bull, J.M., Henstock, T.J., 2008. Evolution of the offshore western Gulf of Corinth. Geol. Soc. Am. Bull. 120, 156–178. https://doi.org/10.1130/B26212.1.
Buckley, J., Hodge, R.A., Slater, L.J., 2024. Bedrock rivers are steep but not narrow: hydrological and lithological controls on river geometry across the USA. Geology 52 (7), 522–526. https://doi.org/10.1130/G51627.1.
Chatanantavet, P., Parker, G., 2008. Experimental study of bedrock channel alluviation under varied sediment supply and hydraulic conditions. Water Resour. Res. 44 (12).
Cook, K.L., Turowski, J.M., Hovius, N., 2013. A demonstration of the importance of bedload transport for fluvial bedrock erosion and knickpoint propagation. Earth Surf. Process. Landf. 38, 683–695. https://doi.org/10.1002/esp.3313.
Cowie, P.A., Whittaker, A.C., Attal, M., Roberts, G., Tucker, G.E., Ganas, A., 2008. New constraints on sediment-flux–dependent river incision: implications for extracting tectonic signals from river profiles. Geology 36, 535. https://doi.org/10.1130/G24681A.1.
de Gelder, G., Fernández-Blanco, D., Melnick, D., Duclaux, G., Bell, R.E., Jara-Muñoz, J., Armijo, R., Lacassin, R., 2019. Lithospheric flexure and rheology determined by climate cycle markers in the Corinth Rift. Sci. Rep. 9, 4260. https://doi.org/10.1038/s41598-018-36377-1.
Deiss, N., Rohais, S., Regard, V., Armitage, J.J., Carretier, S., Bonnet, S., 2025. Source-to-sink signal propagation in a small, coupled catchment-deep-sea fan system: the Sithas example from the Corinth Rift (Pleistocene, Greece). Basin Res. 37, e70044. https://doi.org/10.1111/bre.70044.
Fernández-Blanco, D., de Gelder, G., Lacassin, R., Armijo, R., 2020. Geometry of flexural uplift by continental rifting in Corinth, Greece. Tectonics 39. https://doi.org/10.1029/2019TC005685.
Finnegan, N.J., Roe, G., Montgomery, D.R., Hallet, B., 2005. Controls on the channel width of rivers: implications for modeling fluvial incision of bedrock. Geology 33 (3), 229–232. https://doi.org/10.1130/G21171.1.
Finnegan, N.J., Klier, R.A., Johnstone, S., Pfeiffer, A.M., Johnson, K., 2017. Field evidence for the control of grain size and sediment supply on steady-state bedrock river channel slopes in a tectonically active setting. Earth Surf. Process. Landf. 42, 2338–2349. https://doi.org/10.1002/esp.4187.
Gallen, S.F., Wegmann, K.W., Bohnenstieh, D.R., 2013. Miocene rejuvenation of topographic relief in the southern Appalachians. GSA Today 23, 4–10. https://doi.org/10.1130/GSATG163A.1.
Hobley, D.E.J., Sinclair, H.D., Mudd, S.M., Cowie, P.A., 2011. Field calibration of sediment flux dependent river incision. J. Geophys. Res 116, F04017. https://doi.org/10.1029/2010JF001935.
Humphrey, N.F., Konrad, S.K., 2000. River incision or diversion in response to bedrock uplift. Geology 28 (1), 43–46. https://doi.org/10.1130/0091-7613(2000)28<43:RIODIR>2.0.CO;2.

Jansen, J.D., Fabel, D., Bishop, P., Xu, S., Schnabel, C., Codilean, A.T., 2011. Does decreasing paraglacial sediment supply slow knickpoint retreat? Geology 39 (6), 543–546. https://doi.org/10.1130/G32018.1.

Johnson, J.P.L., Whipple, K.X., 2010. Evaluating the controls of shear stress, sediment supply, alluvial cover, and channel morphology on experimental bedrock incision rate. J. Geophys. Res. 115. https://doi.org/10.1029/2009JF001335, 2009JF001335.

Johnson, J.P.L., Whipple, K.X., Sklar, L.S., Hanks, T.C., 2009. Transport slopes, sediment cover, and bedrock channel incision in the Henry Mountains, Utah. J. Geophys. Res. 114. https://doi.org/10.1029/2007JF000862, 2007JF000862.

Kirby, E., Whipple, K., Harkins, N., 2008. Topography reveals seismic hazard. Nat. Geosci. 1, 485–487. https://doi.org/10.1038/ngeo265.

Lavé, J., Avouac, J.P., 2001. Fluvial incision and tectonic uplift across the Himalayas of central Nepal. J. Geophys. Res. 106, 26561–26591. https://doi.org/10.1029/2001JB000359.

Leonard, J.S., Whipple, K.X., Heimsath, A.M., 2023. Isolating climatic, tectonic, and lithologic controls on mountain landscape evolution. Sci. Adv. 9. https://doi.org/10.1126/sciadv.add8915 eadd8915.

McLeod, J.S., Whittaker, A.C., Bell, R.E., Hampson, G.J., Watkins, S.E., Brooke, S.A.S., Rezwan, N., Hook, J., Zondervan, J.R., Ganti, V., Lyster, S.J., 2024. Landscapes on the edge: river intermittency in a warming world. Geology. https://doi.org/10.1130/G52043.1.

Meyer-Peter, E., Müller, R., 1948. Formulas for bed-load transport. Proceedings of the 2nd Meeting of the International Association for Hydraulic Structures Research, pp. 39–64.

Palyvos, N., Mancini, M., Sorel, D., Lemeille, F., Pantosti, D., Julia, R., Triantaphyllou, M., De Martini, P.-M., 2010. Geomorphological, stratigraphic and geochronological evidence of fast pleistocene coastal uplift in the westernmost part of the Corinth Gulf Rift (Greece). Geol. J. 45, 78–104. https://doi.org/10.1002/gj.1171.

Sklar, L.S., Dietrich, W.E., 2001. Sediment and rock strength controls on river incision into bedrock. Geology 29, 1087. https://doi.org/10.1130/0091-7613(2001)029<1087:SARSCO>2.0.CO;2.

Sklar, L.S., Dietrich, W.E., 2004. A mechanistic model for river incision into bedrock by saltating bed load. Water Resour. Res. 40. https://doi.org/10.1029/2003WR002496.

Sklar, L.S., Dietrich, W.E., 2006. The role of sediment in controlling steady-state bedrock channel slope: implications of the saltation–abrasion incision model. Geomorphology 82, 58–83. https://doi.org/10.1016/j.geomorph.2005.08.019.

Turowski, J.M., Lague, D., Hovius, N., 2007. Cover effect in bedrock abrasion: a new derivation and its implications for the modeling of bedrock channel morphology. J. Geophys. Res. 112. https://doi.org/10.1029/2006JF000697, 2006JF000697.

Turowski, J.M., Hovius, N., Meng-Long, H., Lague, D., Men-Chiang, C., 2008. Distribution of erosion across bedrock channels. Earth Surf. Process. Landf. 33, 353–363. https://doi.org/10.1002/esp.1559.

Turowski, J.M., Lague, D., Hovius, N., 2009. Response of bedrock channel width to tectonic forcing: insights from a numerical model, theoretical considerations, and comparison with field data. J. Geophys. Res. 114, F03016. https://doi.org/10.1029/2008JF001133.

Whipple, K.X., Tucker, G.E., 1999. Dynamics of the stream-power river incision model: implications for height limits of mountain ranges, landscape response timescales, and research needs. J. Geophys. Res 104, 17661–17674. https://doi.org/10.1029/1999JB900120.

Whipple, K.X., Tucker, G.E., 2002. Implications of sediment-flux-dependent river incision models for landscape evolution. J. Geophys. Res 107, 2039. https://doi.org/10.1029/2000JB000044.

Whipple, K.X., DiBiase, R.A., Crosby, B.T., 2013. Bedrock Rivers. Treatise on Geomorphology. Elsevier, pp. 550–573. https://doi.org/10.1016/B978-0-12-374739-6.00254-2.

Whittaker, A.C., Cowie, P.A., Attal, M., Tucker, G.E., Roberts, G.P., 2007. Contrasting transient and steady-state rivers crossing active normal faults: new field observations from the Central Apennines. Italy. Basin Res. 19, 529–556. https://doi.org/10.1111/j.1365-2117.2007.00337.x.

Wicker, V., Ford, M., Gawthorpe, R.L., Skourtsos, E., Kranis, H.D., Kerouédan, L., Muravchik, M., 2024. Transition from late-miocene syn-orogenic extension to plio-pleistocene Corinth rifting in the southern Hellenides, Northern Peloponnese, Greece. Tectonics. 43. https://doi.org/10.1029/2023TC007964 e2023TC007964.

Wobus, C.W., Tucker, G.E., Anderson, R.S., 2006. Self-formed bedrock channels. Geophys. Res. Lett. 33. https://doi.org/10.1029/2006GL027182, 2006GL027182.

Yamanishi, N., Naruse, H., 2026. Limited influence of bedrock strength on river profiles: the dominant role of sediment dynamics. Earth Surf. Dyn. 14 (2), 247–268.

Yanites, B.J., Tucker, G.E., 2010. Controls and limits on bedrock channel geometry. J. Geophys. Res. 115. https://doi.org/10.1029/2009JF001601, 2009JF001601.

Yanites, B.J., Tucker, G.E., Mueller, K.J., Chen, Y.-G., Wilcox, T., Huang, S.-Y., Shi, K.-W., 2010. Incision and channel morphology across active structures along the Peikang River, central Taiwan: implications for the importance of channel width. Geol. Soc. Am. Bull. 122, 1192–1208. https://doi.org/10.1130/B30035.1.

Yanites, B.J., 2018. The dynamics of channel slope, width, and sediment in actively eroding Bedrock River systems. J. Geophys. Res. Earth Surf. 123, 1504–1527. https://doi.org/10.1029/2017JF004405.

Zhang, L., Li, T., Wang, G., Kwang, J.S., Nittrouer, J.A., Fu, X., Parker, G., 2020. How canyons evolve by incision into bedrock: rainbow Canyon, Death Valley National Park, United States. Proc. Natl. Acad. Sci. 117 (26), 14730–14737.

Zhou, Z., Whittaker, A.C., Bell, R.E., Hampson, G.J., 2024. Unravelling tectonic and lithological effects on transient landscapes in the Gulf of Corinth, Greece. Basin Res. 36, e12901. https://doi.org/10.1111/bre.12901.

Zhou, Z., Whittaker, A.C., Bell, R.E., Hampson, G.J., Chandresh, R., Watkins, S.E., Zondervan, J.R., 2026. Decoding tectonic and lithological controls on sediment exported from footwall catchments: implications for hangingwall stratigraphy. Geol. Soc. Am. Bull. https://doi.org/10.1130/B38399.1.

Zondervan, J.R., Whittaker, A.C., Bell, R.E., Watkins, S.E., Brooke, S.A.S., Hann, M.G., 2020. New constraints on bedrock erodibility and landscape response times upstream of an active fault. Geomorphology 351, 106937. https://doi.org/10.1016/j.geomorph.2019.106937.